A major histocompatibility complex class I–dependent subset of memory phenotype CD8+ cells

Onur Boyman,[1,2,3] Jae-Ho Cho,[1,4] Joyce T. Tan,[1] Charles D. Surh,[1] and Jonathan Sprent[1,4]

[1]Department of Immunology, The Scripps Research Institute, La Jolla, CA 92037
[2]Division of Immunology and Allergy, University Hospital of Lausanne, CH-1011 Lausanne, Switzerland
[3]Ludwig Institute for Cancer Research, Lausanne Branch, University of Lausanne, CH-1066 Epalinges, Switzerland
[4]Garvan Institute of Medical Research, Darlinghurst NSW 2010, Australia

Most memory phenotype (MP) CD44hi CD8+ cells are resting interleukin (IL)–15–dependent cells characterized by high expression of the IL–2/IL–15 receptor β (CD122). However, some MP CD8+ cells have a CD122lo phenotype and are IL–15 independent. Here, evidence is presented that the CD122lo subset of MP CD8+ cells is controlled largely by major histocompatibility complex (MHC) class I molecules. Many of these cells display surface markers typical of recently activated T cells (CD62Llo, CD69hi, CD43hi, and CD127lo) and show a high rate of background proliferation. Cells with this phenotype are highly enriched in common γ chain–deficient mice and absent from MHC-I−/− mice. Unlike CD122hi CD8+ cells, CD122lo MP CD8+ cells survive poorly after transfer to MHC-I−/− hosts and cease to proliferate. Although distinctly different from typical antigen–specific memory cells, CD122lo MP CD8+ cells closely resemble the antigen–dependent memory CD8+ cells found in chronic viral infections.

CORRESPONDENCE
Jonathan Sprent:
j.sprent@garvan.org.au

Abbreviations used: MP, memory phenotype; tg, transgenic.

Depending on their stage of differentiation, mature T cells require contact with peptide/MHC complexes and/or cytokines, most notably the common γ chain (γc) cytokines IL-7 and IL-15 (1–4). Naive CD4+ T cells show low expression of CD44, and these CD44lo cells are controlled by IL-7 and possibly MHC-II molecules, although the importance of the latter is controversial (5–7). The factors controlling naturally occurring memory phenotype (MP) CD44hi CD4+ are not well characterized, although antigen-specific memory CD4+ cells are known to be sustained by IL-7 and, to a lesser extent, IL-15 (8–10). For CD8+ cells, naive CD44lo cells are maintained by IL-7 and MHC-I molecules (5, 11, 12), whereas MP and antigen-specific memory cells are controlled by IL-15 and IL-7 and do not require contact with MHC-I complexes (13–16).

For naive T cells, TCR contact with foreign antigen causes CD44lo cells to convert to CD44hi cells and show transient up-regulation

of several surface markers, including IL-2Rα (CD25), CD69, and CD43 (1–4). Many of the responding cells also show decreased levels of CD62L (L-selectin) and IL-7Rα (CD127). Interestingly, naive T cells normally maintain a resting (CD25lo, CD69lo, CD43lo, CD62Lhi, CD127hi) phenotype despite continuous TCR contact with self-MHC ligands, implying that this form of TCR–MHC interaction delivers only a weak signal, adequate for maintaining cell viability but insufficient for overt stimulation and subsequent proliferation. Except for their CD44hi phenotype, MP CD8+ cells show a similar pattern of cell surface markers as naive CD8+ cells, with the exception that ∼60–70% of MP CD8+ cells display high levels of the IL-2/IL-15Rβ chain (CD122). This receptor chain is crucially important for controlling sensitivity to IL-15 (13, 17). Thus, CD122hi MP CD8+ cells are overrepresented in IL-15 transgenic (tg) mice (18, 19). Conversely, IL-15−/− (13, 20) and IL-15Rα−/− (21) mice show a marked and selective reduction of CD122hi MP CD8+ cells. This subset of MP CD8+ cells is highly dependent on IL-15 for IFN-induced bystander proliferation as well as for normal

"background" proliferation (turnover) and survival (13). In marked contrast, the remaining ~30–40% of MP CD8^{+} cells are CD122^{lo} and IL-15 independent. As a consequence, CD122^{lo} MP CD8^{+} cells account for nearly all of the remaining MP CD8^{+} cells in IL-15^{−/−} mice. These cells are unaffected by IFN-induced (IL-15–mediated) bystander proliferation and survive well upon adoptive transfer to IL-15^{−/−} mice (13). We decided to investigate the factor(s) responsible for the survival and turnover of the CD122^{lo} subset of MP CD8^{+} cells.

Here, we demonstrate that the majority of CD122^{lo} MP CD8^{+} cells are a unique population with the phenotype of activated cells. These cells account for most of the residual CD8^{+} cells in γ$_c$[−/−] mice, implying lack of dependence on γ$_c$ cytokines (IL-2, IL-4, IL-7, IL-9, IL-15, and IL-21) for their survival and turnover. Significantly, CD122^{lo} MP CD8^{+} cells disappear rapidly and cease to proliferate upon transfer to MHC-I^{−/−} hosts. Hence, unlike typical IL-15–dependent CD122^{hi} cells, the CD122^{lo} subset of MP CD8^{+} cells is largely cytokine independent and kept alive through continuous TCR contact with MHC-I ligands.

RESULTS

Phenotypic features of MP CD8^{+} subsets

Normal animals accumulate CD44^{hi} MP CD4^{+} and CD8^{+} cells with increasing age, presumably as a result of lifetime exposure to various environmental antigens or self-antigens. In young (2–3-mo-old) C57BL/6 (B6) mice, MP T cells account for ~10% of the T cells in the LN and ~15% of splenic T cells (Fig. 1 A). Although CD44 levels are comparable on MP CD4^{+} and MP CD8^{+} cells, expression of the IL-2/IL-15Rβ receptor (CD122) is considerably higher on MP CD8^{+} than MP CD4^{+} cells, as described previously (13, 17). Thus, plotting CD44 against CD122 divides CD8^{+} cells into three subsets: CD122^{lo} CD44^{lo} (naive), CD122^{lo} CD44^{hi} MP, and CD122^{hi} CD44^{hi} MP cells.

The majority of MP CD8^{+} cells (~60–70%) carries high levels of CD122 (Fig. 1 A). Staining for other surface markers showed that CD122^{hi} MP CD8^{+} cells were quite similar to naive CD44^{lo} CD8^{+} cells for several markers; thus, both subsets consisted almost exclusively of resting T cells characterized by a CD25^{lo}, CD43^{lo}, CD62L^{hi}, CD69^{lo}, and CD127^{hi} phenotype (Fig. 1 B). As shown previously for total MP CD8^{+} cells (22), CD122^{hi} MP CD8^{+} cells differed from naive CD44^{lo} cells in showing a significant but slow tempo of proliferation, as measured by incorporation of the DNA precursor BrdU given for 3 or 7 d (Fig. 1 C). Note that proliferation of CD44^{lo} cells is restricted to BrdU[intermediate] cells, which are recent thymic emigrants that incorporated a low level of BrdU in the thymus before export (22). Despite their similar surface markers, CD122^{hi} MP CD8^{+} cells and naive CD8^{+} cells were clearly different with regard to Bcl-2 expression and IFN-γ production. Thus, relative to naive CD8^{+} cells, CD122^{hi} MP CD8^{+} cells showed two- to three-fold higher levels of Bcl-2 (Fig. 1 D) and >10-fold higher production of IFN-γ upon in vitro stimulation (Fig. 1 E).
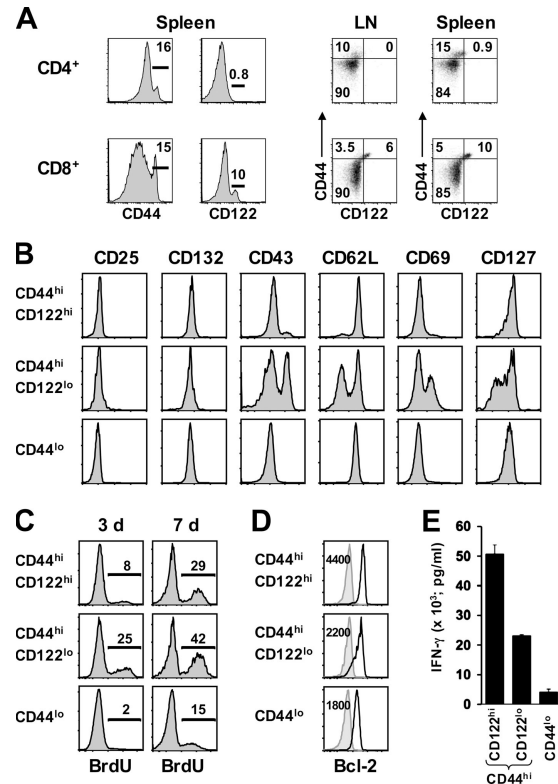

Figure 1. Features of MP CD8^{+} subsets. Spleen and pooled LN cells from 2–3-mo-old normal B6 mice were stained and analyzed by flow cytometry for (A) CD44 and CD122 expression in CD4^{+} or CD8^{+} cells, (B) surface expression of CD25 (IL-2Rα), CD132 (γ$_c$), CD43 (1B11), CD62L (L-selectin), CD69, and CD127 (IL-7Rα) in CD8^{+} T cell subsets, (C) BrdU incorporation of CD8^{+} T cell subsets after 3 or 7 d of BrdU in the drinking water, or (D) intracellular levels of Bcl-2 (solid line) versus isotype-matched control mAb (shaded area) in CD8^{+} T cell subsets. Numbers indicate percentages of gated cells for histograms in A and C, cells in quadrants for dot plots in A, or mean fluorescence intensity of Bcl-2 staining in D. The data are representative of at least three different experiments. (E) CD8^{+} T cell subsets were purified by flow cytometry and stimulated in vitro with PMA and ionomycin for 4 h. Culture supernatants were then collected and assayed by ELISA for IFN-γ. The mean IFN-γ concentrations (plus one standard deviation) are shown. The data are representative of two different experiments.

The properties of the CD122^{lo} subset of CD8^{+} MP cells were quite different. Thus, these cells differed from the other two CD8^{+} subsets in that they were enriched for partly activated cells with a CD43^{hi}, CD62L^{lo}, CD69^{hi}, CD127^{lo} phenotype (Fig. 1 B), thereby resembling TCR-activated T cells (Fig. S1, available at http://www.jem.org/cgi/content/full/jem.20052495/DC1). CD122^{lo} MP cells also showed low levels of Bcl-2 (Fig. 1 D). However, unlike overtly activated T cells stimulated by strong TCR ligation, the levels of CD25 (IL-2Rα) and CD132 (γ$_c$) on CD122^{lo} MP CD8^{+} cells were not elevated (relative to resting T cells). In line with their expression of activation markers, CD122^{lo} MP CD8^{+} cells divided two to three times faster than the CD122^{hi} MP CD8^{+} subset (Fig. 1 C). Also, CD122^{lo} CD44^{hi} CD8^{+} cells produced

twofold less IFN-γ than the CD122^{hi} subset of MP CD8$^+$ cells (Fig. 1 E), suggestive of partial anergy.

Collectively, the data described above indicate that MP CD8$^+$ cells can be divided into resting CD122^{hi} cells and partly activated CD122^{lo} cells. Nevertheless, some of the CD122^{lo} cells seemed to be resting cells. The origin of these latter cells is discussed below.

Adoptive transfer of CD8$^+$ cell subsets to normal B6 mice

The properties of the activated CD122^{lo} subset of MP CD8$^+$ cells suggested that these cells could be a short-lived population. To investigate this possibility, we purified CD8$^+$ cell subsets by FACS. The purity of the CD8$^+$ subsets after sorting was usually >99% for CD44^{lo} cells and CD122^{hi} CD44^{hi} cells, and 88–90% for the CD122^{lo} CD44^{hi} subset (Fig. 2 A). The sorted CD8$^+$ subsets were prepared from Thy1.1 congenic mice and adoptively transferred i.v. to normal young B6 mice (Thy1.2). The host mice were killed 7 d later to analyze LN and spleen cells by flow cytometry. The transferred CD44^{lo} CD8$^+$ cells accumulated preferentially in host LN, and most (>96%) of the cells maintained low levels of CD44, thus maintaining their naive phenotype (Fig. 2 B). The transferred CD122^{hi} MP CD8$^+$ cells homed equally well to the LN and spleen. Interestingly, the cells recovered from host LN were >95% CD122^{hi}, whereas ∼30% of the cells from the spleen were CD122^{lo} cells, suggestive of CD122 downregulation (see below). These latter CD122^{lo} cells maintained their CD62L^{hi} phenotype (Fig. 2 C) and did not express the activation markers discussed above (not depicted).

The transferred CD44^{hi} CD122^{lo} CD8$^+$ cells behaved differently. These cells homed preferentially to the spleen and a considerable fraction partly up-regulated CD122, both in the LN and spleen. As seen above for BrdU incorporation, the transferred MP CD122^{lo} CD8$^+$ cells proliferated considerably, yielding two- to threefold higher cell recoveries than for transferred CD122^{hi} MP cells or CD44^{lo} cells, especially in the spleen (Fig. 2, B and D). Like the initially injected cells, many of the recovered cells maintained a CD62L^{lo} phenotype (Fig. 2 C), contrasting with the CD122^{lo} cells derived from the transferred MP CD122^{hi} CD8$^+$ cells that were purely CD62L^{hi}. Upon CD122 up-regulation, however, the transferred CD44^{hi} CD122^{lo} CD8$^+$ cells became predominantly CD62L^{hi} (Fig. 2 C).

Therefore, the transfer experiments described above suggest that the CD122^{lo} subset of MP CD8$^+$ cells consists of a mixture of (a) partly activated cells and (b) resting MP cells that down-regulated their CD122 levels, perhaps in response to IL-15. In favor of this idea, brief (∼4 h) exposure of normal CD8$^+$ cells to IL-15 in vitro at 37°C caused CD122^{hi} cells to revert to CD122^{lo} cells while remaining CD62L^{hi} (Fig. S2, available at http://www.jem.org/cgi/content/full/jem.20052495/DC1).

CD8$^+$ cell subsets in $\gamma_c^{-/-}$ mice

As mentioned above, MP CD8$^+$ cells in IL-15$^{-/-}$ and IL-15R$\alpha^{-/-}$ mice are nearly all CD122^{lo} cells (13, 20, 21, and
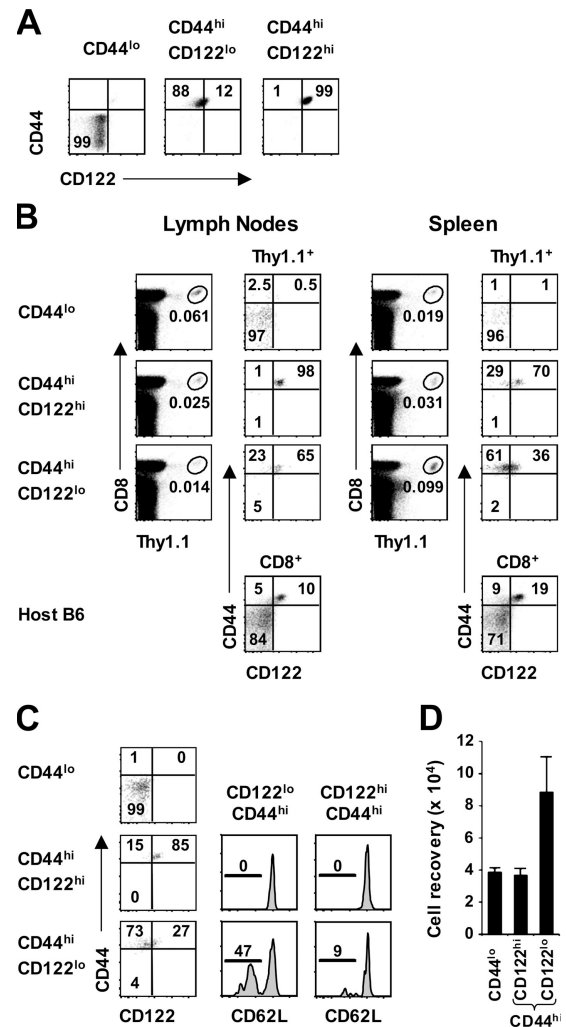

Figure 2.   Phenotype of MP CD8$^+$ cells on adoptive transfer.
(A) Thy1.1-marked pooled LN cells from normal B6 mice were sorted by flow cytometry for CD44^{lo} versus CD44^{hi} CD122^{lo} versus CD44^{hi} CD122^{hi} CD8$^+$ T cells, resulting in the indicated purities after the sort. Sorted CD8$^+$ T cell subsets were then transferred i.v. at 1.5 × 10^6 cells/mouse to Thy1.2-marked WT mice, recovered 7 d later from pooled LN and spleen cells, and stained for FACS analysis. Transferred donor cells, identified as CD8$^+$ Thy1.1$^+$ cells, were examined for (B and C, left) CD44 versus CD122 and CD62L expression levels in CD44^{hi} CD122^{lo} (C, middle) versus CD44^{hi} CD122^{hi} donor CD8$^+$ cells (C, right). The CD44/CD122 gates were set according to host CD8$^+$ cells in the same staining as shown. Numbers indicate percentages of cells in quadrants. (D) Total donor cell numbers (plus one standard deviation) were calculated for mice in B. The data show total numbers of donor-derived T cells recovered from the spleens and pooled LNs of host mice (two mice/group) after injection of purified donor CD44^{lo}, CD44^{hi} CD122^{hi}, and CD44^{hi} CD122^{lo} CD8$^+$ cells. The data are representative of at least two separate experiments.

unpublished data). Interestingly, the few CD8$^+$ cells present in $\gamma_c^{-/-}$ mice proved to be CD122^{lo} cells (Fig. 3 A). These cells comprised a relatively homogeneous population with high intermediate expression of CD44 and low intermediate expression of CD122. Like MP CD8$^+$ cells from

IL-15$^{-/-}$ mice, $\gamma_c$$^{-/-}$ CD8$^+$ cells were enriched for activation markers (Fig. 3 C and not depicted) and had a rapid turnover (Fig. 3 D).

These findings with $\gamma_c$$^{-/-}$ CD8$^+$ cells suggested that the CD122^{lo} MP CD8$^+$ cells in normal mice may be independent of γ_c cytokines. If so, raising the level of γ_c cytokines would be expected to expand only the CD122^{hi} and not the CD122^{lo} subset of CD8$^+$ cells. In line with this prediction, CD122^{lo} cells comprised only a small proportion of MP CD8$^+$ cells in mice expressing high levels of γ_c cytokines, namely IL-7 tg mice (Fig. 3 B; reference 14). In these mice, $\sim$90% of MP CD8$^+$ cells were CD122^{hi} cells with a resting phenotype and slow turnover (Fig. 3 D and not depicted).

The enrichment of activated CD122^{lo} MP CD8$^+$ cells in IL-15$^{-/-}$ and $\gamma_c$$^{-/-}$ mice raised the possibility that these cells were not maintained by cytokines but by other stimuli, perhaps TCR interactions with MHC-I ligands. Indirect support for this possibility came from the finding that MHC-I$^{-/-}$ mice were virtually devoid of CD122^{lo} MP CD8$^+$ cells (Fig. 3 A). These mice contained MP CD8$^+$ cells, presumably selected by MHC-Ib molecules (23), but these cells consisted almost entirely of CD122^{hi} cells with a resting phenotype and slow turnover (Fig. 3, C and D).

Transfer of CD122$^{-/-}$ MP CD8$^+$ cells to MHC-I$^{-/-}$ hosts

Collectively, the data described above suggest that γ_c cytokines are not essential for survival or background turnover of

Figure 3. MP CD8$^+$ subsets in $\gamma_c$$^{-/-}$ and MHC-I$^{-/-}$ mice. Spleen cells from age- and gender-matched (A) WT, $\gamma_c$$^{-/-}$, or MHC-I$^{-/-}$ mice, or (B) WT and IL-7 tg mice (all on a B6 background) were stained for CD3, CD8α, CD44, and CD122 and analyzed by flow cytometry for CD44 and CD122 expression levels on CD8$^+$ T cells. The CD8$^+$ cells in MHC-I$^{-/-}$ mice were additionally stained for CD8β and TCRβ to confirm that these cells were CD8$\alpha\beta^+$ TCR$\alpha\beta^+$ cells. Numbers indicate percentages of cells in quadrants. (C) Spleen cells from the indicated mice were stained for CD3, CD8, CD62L, CD43 (top) or CD3, CD8, CD69, and CD43 (bottom) and analyzed by flow cytometry. The data show staining of gated CD3$^+$ CD8$^+$ cells. (D) The indicated mice were given BrdU in the drinking water for 3 d before being killed and intracellular BrdU staining. Shown are the percentages of BrdU$^+$ cells in CD44^{hi} CD122^{lo} or CD44^{hi} CD122^{hi} CD8$^+$ T cells. The data are representative of at least two different experiments.

CD122^{lo} CD44^{hi} CD8$^+$ cells and that these cells might be maintained and stimulated through contact with MHC-I ligands. To examine this possibility directly, we transferred cells to MHC-I$^{-/-}$ hosts. In initial experiments, CD8$^+$ cells were prepared from CD122$^{-/-}$ mice. These mice contain large numbers of CD8$^+$ cells, most (>70%) of which express activation markers and have a rapid turnover (Fig. S3, available at http://www.jem.org/cgi/content/full/jem.20052495/DC1). By these parameters and being CD122$^{-/-}$, the cells closely resemble the CD122^{lo} subset of MP CD8$^+$ cells in normal mice. To test whether these cells are MHC-I dependent, purified total T cells from CD122$^{-/-}$ mice were labeled with CFSE and adoptively transferred to sublethally irradiated (750 cGy) WT versus MHC-I$^{-/-}$ mice. Irradiation of the hosts was necessary to reduce rejection of the transferred cells by the residual MP CD8$^+$ cells in the MHC-I$^{-/-}$ recipients. By 7 d after cell transfer, the donor CD4$^+$ T cells had proliferated comparably well in WT and MHC-I$^{-/-}$ hosts as shown by CFSE dilution (Fig. 4 A). In marked contrast, the donor CD8$^+$ T cells proliferated well in the WT mice but showed almost no division in MHC-I$^{-/-}$ recipients, resulting in 10-fold reduced cell recoveries from MHC-I$^{-/-}$ hosts compared with WT recipients (Fig. 4, A and B).

For the WT hosts, some of the proliferating donor CD8$^+$ cells might be derived from contaminating naive cells, which can undergo MHC-I–dependent lymphopenia-induced proliferation. Therefore, we prepared purified (99%) CD44^{hi} T cells from CD122$^{-/-}$ mice and adoptively transferred these cells to irradiated WT versus MHC-I$^{-/-}$ mice. Again, 7 d after adoptive transfer, the donor CD4$^+$ T cells showed comparable division profiles in both groups as shown by CFSE dilution, whereas the donor CD8$^+$ T cells proliferated much less in MHC-I$^{-/-}$ recipients than in WT hosts (Fig. 4 C). This difference was also seen when the transferred cells were enriched for CD44^{hi} T cells ($\sim$90%) by magnetic cell sorting (Fig. 4 D). In contrast to these experiments using T cells from CD122$^{-/-}$ mice, when sorted CD44^{hi} T cells from normal B6 WT mice were used as donor cells, the donor CD8$^+$ T cells proliferated equally well in both hosts (Fig. 4 E), demonstrating that CD122^{hi} MP CD8$^+$ cells expand in an MHC-I–independent fashion (24).

Thus, these experiments show that proliferation of CD122$^{-/-}$ CD44^{hi} CD8$^+$ cells is heavily dependent on contact with MHC-I molecules.

Transfer of normal MP CD8$^+$ cells to MHC-I$^{-/-}$ hosts

Despite their similar phenotype, MP CD8$^+$ cells from CD122$^{-/-}$ mice might not necessarily be equivalent to the CD122^{lo} subset of MP CD8$^+$ cells in normal mice. Hence, it remained important to test the MHC-I dependency of normal CD122^{lo} MP CD8$^+$ cells. Therefore, the experiments described above were repeated with purified MP CD8$^+$ cells prepared from normal B6 mice. Rather than injecting purified CD122^{lo} MP CD8$^+$ cells, which are difficult to prepare in more than minimal numbers from normal mice (Fig. 2), we transferred purified normal B6 MP CD8$^+$ cells
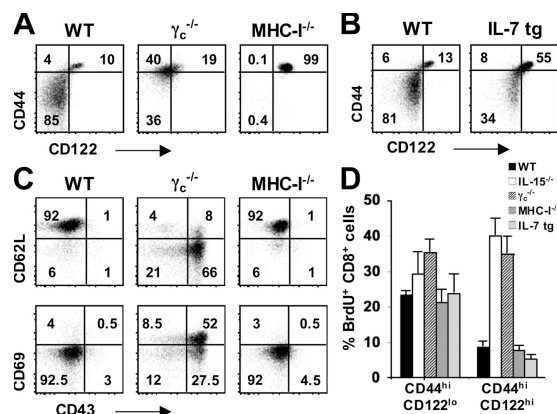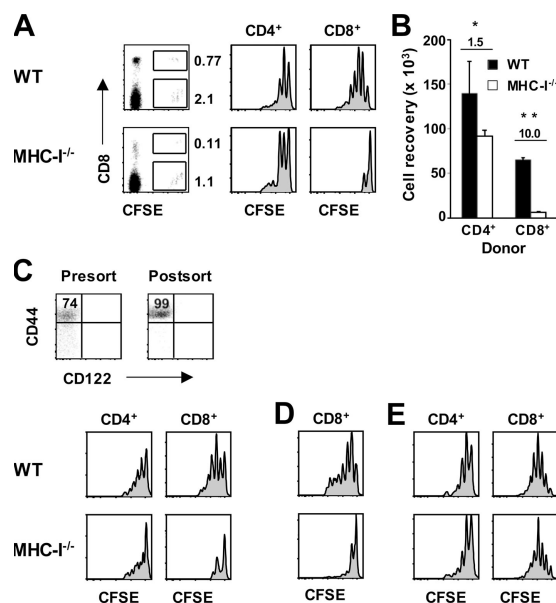
Figure 4. Fate of CD122$^{-/-}$ T cells transferred to irradiated MHC–I$^{-/-}$ hosts. Irradiated WT versus MHC–I$^{-/-}$ hosts were injected i.v. with (A–D) CFSE-labeled T cells (2–3 × 10^6 cells/mouse) from CD122$^{-/-}$ mice or (E) purified and CFSE-labeled CD44^{hi} T cells (2–3 × 10^6 cells/mouse) from normal B6 WT mice. The cells transferred were (A and B) unseparated CD122$^{-/-}$ T cells prepared by complement-mediated killing with mAbs, (C) FACS-sorted CD44^{hi} CD122$^{-/-}$ T cells, (D) CD8$^+$ CD122$^{-/-}$ cells enriched for CD44^{hi} cells by magnetic bead separation, or (E) FACS-sorted CD44^{hi} T cells from normal B6 WT mice. The host mice received (A, B, and E) a single dose of 750 cGy or (C and D) two doses of 600 cGy 2 wk apart. CFSE dilution of the cells recovered from host spleen was examined 7 d later. Histograms show CFSE^{hi} CD4$^+$ or CD8$^+$ donor cells, respectively. Numbers indicate percentages of cells in quadrants. (B) Total cell numbers (plus one standard deviation) of donor CD4$^+$ and CD8$^+$ T cells recovered from the spleens and pooled LNs of WT (filled bars) versus MHC–I$^{-/-}$ (open bars) hosts treated as in A (two mice/group). Numbers above the bars indicate the ratios of total cells from WT versus MHC–I$^{-/-}$ hosts. p-values of WT compared with MHC–I$^{-/-}$ cell numbers were calculated using a paired t test. *, not significant (P = 0.4); **, significant (P = 0.02). The data are representative of at least two different experiments.

(i.e., a mixture of CD122^{lo} CD44^{hi} and CD122^{hi} CD44^{hi} cells) to irradiated WT versus MHC–I$^{-/-}$ hosts (Fig. 5 A). When the injected cells were recovered 1 wk later, a high proportion of the donor CD44^{hi} cells (90%) were CD122^{hi}, presumably reflecting homeostatic expansion of these latter cells in response to the raised levels of γ_c cytokines in the lymphopenic environment of the irradiated hosts (14). The few donor CD122^{lo} cells in the WT hosts were enriched for cells with an activated CD62L^{lo} CD43^{hi} phenotype, consistent with chronic activation to MHC–I ligands (Fig. 5 B). Significantly, cells with this activated phenotype were quite rare in the MHC–I$^{-/-}$ hosts. In these hosts, the donor MP CD8$^+$ cells were enriched for CD122^{hi} cells and the minor subset of donor CD122^{lo} cells had a resting CD62L^{hi} CD43^{lo} phenotype, consistent with these cells being revertants from CD122^{hi} cells (Fig. 5 B). In terms of cell numbers, total numbers of
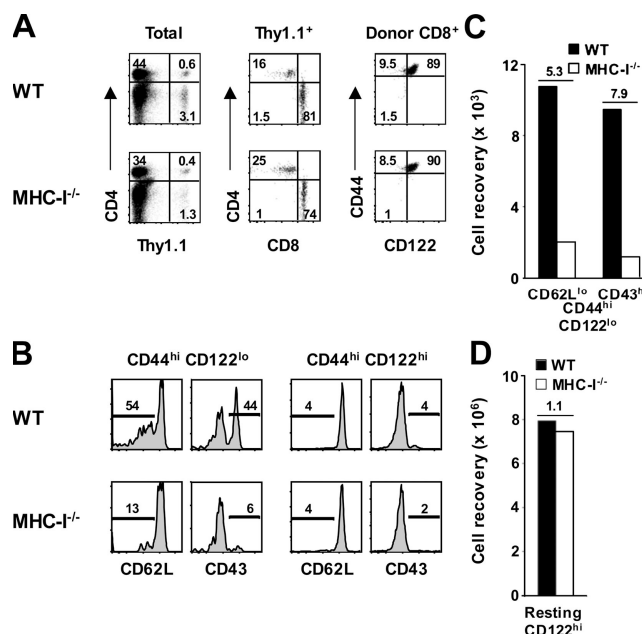
Figure 5. Fate of normal B6 MP T cells transferred to irradiated MHC–I$^{-/-}$ hosts. Purified CD44^{hi} T cells from Thy1.1-marked normal B6 WT mice were transferred i.v. at 1.5 × 10^6 cells/mouse to irradiated (750 cGy) Thy1.2-marked WT or MHC–I$^{-/-}$ mice. 7 d after transfer, mice were killed and analyzed by flow cytometry for donor (Thy1.1$^+$) CD8$^+$ and CD4$^+$ cells (A), and for CD62L and CD43 expression on donor CD122^{lo} CD44^{hi} CD8$^+$ (B, left two columns) versus CD122^{hi} CD44^{hi} CD8$^+$ cells (B, right two columns). Total numbers of donor CD44^{hi} CD8$^+$ T cells were calculated and are shown for (C) CD122^{lo} CD62L^{lo} and CD122^{lo} CD43^{hi} cells, and (D) CD122^{hi} CD62L^{hi} CD43^{lo} cells (resting CD122^{hi} cells) recovered from the spleens and pooled LNs of WT (filled bars) versus MHC–I$^{-/-}$ (open bars) hosts. Numbers above the bars indicate the ratios of total cells from WT versus MHC–I$^{-/-}$ hosts. The data are representative of at least two separate experiments.

CD62L^{lo} and CD43^{hi} subsets of donor CD44^{hi} CD122^{lo} CD8$^+$ cells were greatly reduced in MHC–I$^{-/-}$ hosts; i.e., by fivefold and eightfold, respectively (Fig. 5 C). In contrast, total numbers of donor CD122^{hi} cells in WT and MHC–I$^{-/-}$ hosts were comparable (Fig. 5 D).

The above findings indicated that as for CD8$^+$ cells from CD122$^{-/-}$ mice, the subset of activated CD122^{lo} MP CD8$^+$ cells in normal mice disappeared rapidly after transfer to MHC–I$^{-/-}$ hosts.

Transfer to nonirradiated MHC–I$^{-/-}$ hosts

A complicating feature of the experiments described above is that irradiation of the hosts to prevent rejection caused the donor cells to undergo lymphopenia-induced homeostatic proliferation. Hence, it was important to have comparable information on cell survival in nonirradiated MHC–I$^{-/-}$ hosts. Here, the main problem is rejection by residual host CD8$^+$ cells. Because rejection by MHC–I$^{-/-}$ hosts is directed to MHC–I molecules on the donor cells, we avoided the problem of rejection by preparing donor cells that lacked MHC–I; i.e., by reconstituting heavily irradiated normal B6 WT mice
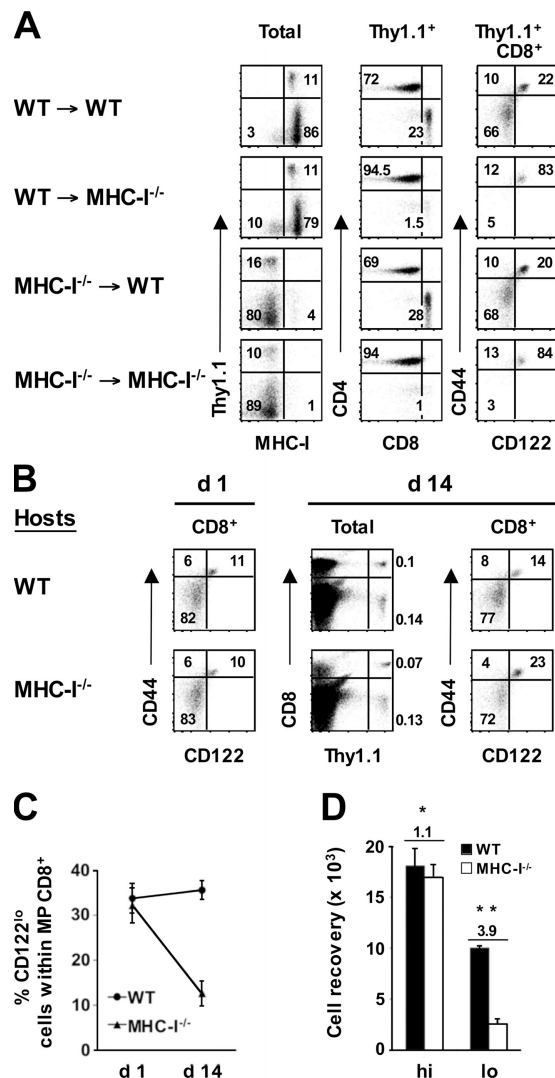
Figure 6. Fate of MHC-I$^{-/-}$ chimera T cells transferred to non-irradiated MHC-I$^{-/-}$ hosts. (A) BM chimeras were prepared by transferring BM stem cells (BM cells depleted of mature B, T, and MHC-II–expressing cells by mAb plus complement) to lethally irradiated (1,300 cGy) Thy1.2-marked WT or MHC-I$^{-/-}$ mice. The data show representative staining for T cell subsets in the spleens of the indicated chimeras at 3–4 mo after reconstitution. (B and C) Purified MHC-I$^{-/-}$ T cells (Thy1.1$^+$) from MHC-I$^{-/-}$→WT BM chimeras were adoptively transferred i.v. at 2–3 × 10^6 cells/mouse to Thy1.2-marked WT or MHC-I$^{-/-}$ mice, which had been depleted of NK cells using anti-NK1.1 mAb (PK136) on days −3 and −1 before adoptive transfer and every other day thereafter. On days 1 and 14 after adoptive transfer, mice were killed and phenotyped by flow cytometry for the presence of donor CD8$^+$ subsets (B), or the percentage of donor CD122^{lo} CD44^{hi} CD8$^+$ cells within total donor CD44^{hi} CD8$^+$ cells was calculated (C). Numbers in A and B indicate percentages of cells in quadrants. (D) Total cell numbers (plus one standard deviation) of donor CD44^{hi} CD8$^+$ T cells, which were CD122^{hi} (hi) or CD122^{lo} (lo), recovered from the spleens and pooled LNs of WT (filled bars) versus MHC-I$^{-/-}$ (open bars) hosts from two independent experiments performed as described in B. Numbers above the bars indicate the ratios of cell numbers recovered from WT versus MHC-I$^{-/-}$ hosts. p-values of WT compared with MHC-I$^{-/-}$ cell numbers were calculated using a paired *t* test. *, not significant (P = 0.2); **, significant (P = 0.04).

with BM cells from MHC-I$^{-/-}$ mice (25). The MHC-I$^{-/-}$ CD4$^+$ and CD8$^+$ cells generated in these MHC-I$^{-/-}$→WT chimeras closely resembled the cells generated in control WT→WT chimeras (Fig. 6 A). In contrast, CD4$^+$ cells, but very few CD8$^+$ cells, were generated in reciprocal WT→MHC-I$^{-/-}$ and MHC-I$^{-/-}$→MHC-I$^{-/-}$ chimeras.

For adoptive transfer experiments, we used purified donor Thy1-marked T cells from MHC-I$^{-/-}$ (Thy1.1)→WT (Thy1.2) chimeras. These MHC-I$^{-/-}$ T cells, a mixture of CD4$^+$ and CD8$^+$ cells, were then transferred to WT versus MHC-I$^{-/-}$ mice (both Thy1.2). To avoid rejection by NK cells, the hosts had been pretreated with anti–NK1.1 mAb. With transfer to WT hosts, the phenotype of the donor MP CD8$^+$ cells remained constant and there was no decline in the proportion of CD122^{lo} cells (Fig. 6 B). With transfer to MHC-I$^{-/-}$ hosts, in contrast, the proportion of CD122^{lo} MP CD8$^+$ cells declined abruptly between days 1 and 14 after transfer, leading to a reciprocal relative increase in CD122^{hi} cells (Fig. 6 C). This decrease in CD122^{lo} MP CD8$^+$ donor cells was also evident from total cell recoveries after adoptive transfer. Thus, for the donor MP CD8$^+$ cells, the total recovery of CD122^{hi} cells was the same in WT and MHC-I$^{-/-}$ hosts on day 14, whereas the recovery of CD122^{lo} cells was fourfold lower in MHC-I$^{-/-}$ hosts than in WT hosts (Fig. 6 D). There was no change in CD4$^+$ cells (not depicted).

Collectively, the above three sets of experiments with MHC-I$^{-/-}$ hosts indicate that the subset of MP CD8$^+$ cells with an activated CD122^{lo} phenotype is MHC-I dependent and is presumably engaged in chronic TCR responses to MHC-I ligands.

DISCUSSION

As mentioned earlier, T cells exhibiting the properties and features of antigen-specific memory cells arise early in life and become a dominant population in old age. The prevailing view is that these naturally occurring MP T cells are the progeny of naive precursors responding to various environmental antigens. However, some MP T cells may arise through contact with self-antigens rather than foreign antigens. This possibility is supported by the finding that naive T cells undergo "homeostatic" proliferation and differentiation into typical MP cells during T lymphopenia, e.g., in the normal neonatal period or when adult mice are depleted of T cells (26–28). This proliferative response is directed largely to self-antigens and is stimulated by the raised levels of γ_c cytokines, especially IL-7, that occur when total T cell levels are low. What proportion of MP cells are driven by self-rather than foreign antigens in normal mice is unclear. Nevertheless, it is notable that MP cells are readily detectable in germ-free mice and even in "antigen-free" mice fed an amino acid diet (29, 30, 31 and unpublished data). Thus, most MP cells may be the progeny of self-reactive cells. Characterizing the features of MP cells is therefore important.

For MP CD8$^+$ cells, we show here that these cells comprise two broad subsets: (a) a major population of resting CD122^{hi} CD44^{hi} cells and (b) a minor subset of partly activated

CD122^{lo} CD44^{hi} cells. The CD122^{hi} subset closely resembled naive CD44^{lo} CD8$^+$ cells by several surface markers but was distinct in two respects. First, confirming previous findings (13, 22), background proliferation of CD122^{hi} cells was slow but significant; in contrast, naive CD44^{lo} CD8$^+$ cells rarely divided. Second, unlike naive CD8$^+$ cells, CD122^{hi} CD8$^+$ cells proved to be MHC-I independent. Thus, CD122^{hi} cells expanded in MHC-I$^{-/-}$ hosts, whereas naive cells gradually disappeared (Fig. 6 and not depicted).

Unlike CD122^{hi} cells, the CD122^{lo} component of MP CD8$^+$ cells had a rapid turnover and was enriched in cells with activated phenotype. These cells were spread throughout the secondary lymphoid tissues, including peripheral LNs, suggesting the cells were activated by a pervasive rather than a local stimulus. As in IL-15$^{-/-}$ mice, CD122^{lo} MP CD8$^+$ cells were enriched in $\gamma_c^{-/-}$ mice, indicating a lack of dependence on γ_c cytokines. Although reliance on other cytokines cannot be excluded, the cells are probably maintained largely by TCR stimuli. This follows from the finding that CD122^{lo} MP CD8$^+$ cells disappeared rapidly and ceased to proliferate after transfer to MHC-I$^{-/-}$ hosts. It should be noted that a significant proportion of CD122^{lo} MP CD8$^+$ cells (30–50%) were MHC-I independent and had a resting phenotype. Based on the effects of exposing cells to IL-15 in vitro, resting CD122^{lo} MP CD8$^+$ cells are probably "revertants" of CD122^{hi} cells responding to IL-15.

A key issue is whether the activated CD122^{lo} subset of MP cells can be equated with a subset of antigen-specific memory cells. In the case of CD122^{hi} MP CD8$^+$ cells, these cells closely resemble typical long-lived, antigen-specific "central" memory cells (4) by multiple parameters, including surface markers, turnover, IL-15 dependency, and lack of dependence on MHC-I. It might then follow that CD122^{lo} MP CD8$^+$ cells are the counterpart of "effector" memory cells. This is unlikely for several reasons (32–34). First, despite their CD62L^{lo} phenotype, effector memory cells do not display activation markers. Second, whereas CD122^{lo} MP CD8$^+$ cells have a rapid turnover, effector memory CD8$^+$ cells have a slow turnover. Third, in terms of IFN-γ production, CD122^{lo} MP cells are anergic, whereas effector memory cells respond as effectively as central memory cells. Fourth, unlike CD122^{lo} MP cells, effector memory cells are CD122^{hi} cells. Fifth, unlike effector memory cells, CD122^{lo} MP CD8$^+$ cells are proportionally as frequent in LNs as in the spleen. Hence, activated CD122^{lo} MP CD8$^+$ cells cannot be equated with either effector or central memory cells.

Although clearly different from classical memory cells, CD122^{lo} MP CD8$^+$ cells closely resemble a population of antigen-specific memory CD8$^+$ cells that develops during chronic viral infections in mice (35–37). These cells have low levels of CD122, IL-7Rα, CD62L, and Bcl-2, express higher levels of CD43 as well as CD69, and display partial anergy in terms of antigen responsiveness. Significantly, CD8$^+$ cells in chronic infections rapidly disappear when deprived of contact with specific antigen, suggesting that the cells are maintained largely by chronic TCR contact with persisting antigen. Interestingly, CD8$^+$ cells found in HIV-infected individuals are enriched in cells carrying memory markers as well as low levels of IL-7Rα and CD62L, show a higher in vivo proliferation rate, and are more susceptible to apoptosis and partially anergic in vitro (38). Thus, the memory CD8$^+$ cells generated during chronic infection have much in common with the naturally occurring population of CD122^{lo} MP CD8$^+$ cells described here.

The MHC-I ligands recognized by CD122^{lo} MP CD8$^+$ cells are unclear. The possibility we favor is that these cells are reacting to the same self-ligands that drive homeostatic proliferation in lymphopenic hosts. In favor of this hypothesis, we found similar Vβ TCR usage within CD122^{lo} MP CD8$^+$ cells and polyclonal CD8$^+$ T cells undergoing homeostatic expansion (Fig. S4, A and B, available at http://www.jem.org/cgi/content/full/jem.20052495/DC1).

In normal hosts, proliferation to self MHC-I ligands might be limited to a small subset of naive CD8$^+$ cells with "above-average" affinity for self. If so, what is the fate of the responding CD122^{lo} cells? One possibility is that CD122^{lo} cells resemble typical effector cells in having a short lifespan: the cells proliferate in brief but most of the cells then die. However, CD122^{lo} MP CD8$^+$ cells differ from typical effector cells in that they are CD25^{lo} and display partial anergy, at least for IFN-γ synthesis. More importantly, the transfer studies showed that at a population level, purified CD122^{lo} cells did not die but survived quite well in WT hosts, with some of the cells differentiating into CD122^{hi} cells. Hence, the data favor a model in which contact with self–MHC-I ligands drives CD8$^+$ cells to proliferate and then differentiate from semi-activated CD122^{lo} cells into resting CD122^{hi} cells. To maintain homeostasis, cell expansion here is presumably balanced by an equivalent rate of cell death, but how such immunoregulation is controlled is unclear. It is also a mystery that differentiation into CD122^{hi} cells causes CD8$^+$ cells to lose their MHC-I dependency. Future studies will be required to resolve these issues.

MATERIALS AND METHODS

Mice. C57BL/6 (B6), Thy1.1 (B6.PL), CD122-deficient (CD122$^{-/-}$), and γ_c-deficient ($\gamma_c^{-/-}$) mice, all on a B6 background, were purchased from The Jackson Laboratory. D$^{b-/-}$ K$^{b-/-}$ β_2M$^{-/-}$ MHC-I–deficient mice on a B6 background (16) were provided by R. Ahmed (Emory University, Atlanta, GA) and maintained in our animal facility. IL-15–deficient (IL-15$^{-/-}$) mice (13) and IL-7 tg mice (14) were maintained in our animal facility. All mice were housed under specific pathogen-free conditions at The Scripps Research Institute and used at 3–6 mo of age. Experiments involving the use of animals were approved by the Institutional Animal Care and Use Committee at The Scripps Research Institute.

Flow cytometry and cell sorting. Cell suspensions of spleen or pooled (inguinal, axillary, cervical, and mesenteric) LNs were prepared according to standard protocols and stained for FACS analysis or sorting using PBS containing 1% FCS and 2 mM EDTA with the following mAbs (from BD Biosciences unless otherwise stated): PerCP-Cy5.5–conjugated anti-CD3 (145-2C11); Alexa Fluor 405–conjugated anti-CD4 (RM4-5; Caltag Laboratories); PerCP-Cy5.5– or APC-Cy7–conjugated anti-CD8α (53-6.7); PE-conjugated anti-CD8β (H35-17.2); FITC-conjugated anti-CD25 (PC61.5); PE-conjugated anti-CD43 (1B11); APC-conjugated anti-CD44 (IM7; eBioscience); FITC- or PE-conjugated anti-CD62L (MEL-14);

FITC-conjugated anti-CD69 (H1.2F3); APC-conjugated anti-CD90.1 (HIS51; eBioscience); FITC- or PE-conjugated anti-CD122 (TM-β1 or alternatively 5H4); PE-conjugated anti-CD127 (SB/14); and PE-conjugated anti-CD132 (4G3). For staining of the intracellular markers Bcl-2 and BrdU, the Bcl-2 reagent set containing FITC-conjugated anti–Bcl-2 mAb (3F11) or FITC-conjugated isotype-matched control mAb and the FITC BrdU flow kit (both from BD Biosciences) were used, respectively, according to standard protocols (22). In brief, cells were stained for cell surface markers, fixed using 2% paraformaldehyde, and permeabilized using saponin before intracellular staining. Flow cytometry samples were analyzed using a BD LSR II digital flow cytometer. For determining Vβ TCR usage, the Vβ TCR Screening Panel from BD Biosciences was used according to the manufacturer's recommendation.

Measurement of cell turnover in vivo. Proliferation of cells in vivo was measured using dilution of CFSE-labeled cells (13) or incorporation of BrdU (0.8 mg/ml) given in the drinking water (22). CFSE staining was performed as follows: cells were resuspended in PBS containing 1% FCS at $10–20 \times 10^6$ cells/ml and stained with 1 μl of 5 mM Vybrant CFDA SE Cell Tracer kit (Invitrogen) per milliliter of cell suspension for 10 min at 37°C, and then washed twice with ice-cold PBS containing 1% FCS. BrdU staining was performed as described above.

In vitro stimulation and IFN-γ measurement by ELISA. Spleen cells from normal B6 mice were sorted by FACS for $CD44^{lo}$, $CD44^{hi} CD122^{lo}$, and $CD44^{hi} CD122^{hi} CD8^+$ T cells. These purified $CD8^+$ cell subsets were then seeded in a V-bottom 96-well plate in triplicates at 7×10^5 cells/well and stimulated with 50 ng/ml PMA and 500 ng/ml ionomycin for 4 h under standard culture conditions (37°C, 7% CO_2, humidified atmosphere). Supernatants were then collected and assayed for IFN-γ by a sandwich ELISA according to standard protocols, as described previously (39). In brief, culture supernatants were diluted serially in PBS and added to flat-bottom 96-well plates coated with a purified mAb specific for IFN-γ (XMG1.2; eBioscience). Known concentrations of recombinant murine IFN-γ were used as standards. After incubation for 2 h at 37°C, the plates were washed and biotinylated mAb (R4-6A2; eBioscience) was added for 1 h at 37°C. After washing again, streptavidin–conjugated horseradish peroxidase was added for 1 h at room temperature. The samples were then developed using the substrate O-phenylenediamine (Sigma-Aldrich) and, after stopping the reaction with 2 N H_2SO_4, analyzed with an ELISA reader (Spectramax Plus 384; Molecular Devices).

Adoptive transfer of purified CD8+ T cell subsets. Pooled LN cells from Thy1.1-marked WT or IL-7 tg mice were surface stained for CD122, CD8β, and CD44 and sorted using a Becton Dickinson FACS Aria. Purities of FACS-sorted $CD8^+$ T cell subsets were >99% for $CD44^{lo}$, 88–90% for $CD44^{hi} CD122^{lo}$, and >99% for $CD44^{hi} CD122^{hi}$. $CD8^+$ T cell subsets were then transferred i.v. at 1.5×10^6 cells/mouse to Thy1.2-marked WT mice and left for 7 d before mice were killed. IL-7 tg mice were used in some experiments as they contained higher numbers of total spleen and LN cells enriched for $CD44^{hi} CD8^+$ T cells (14), which, divided into $CD122^{lo}$ and $CD122^{hi}$ cells, were indistinguishable from the corresponding subsets in WT mice by all parameters tested (Fig. 3 and unpublished data). For experiments using adoptive transfer of purified $CD44^{hi}$ T cells, pooled LN cells from Thy1.1-marked WT or IL-7 tg mice were FACS sorted (yielding a purity of >98%), labeled with CFSE where indicated, and transferred i.v. at the indicated cell numbers/mouse to sublethally irradiated (750 cGy) Thy1.2-marked WT or MHC-I$^{-/-}$ mice. 7 d after transfer, mice were killed and analyzed by flow cytometry.

Adoptive transfer of purified CD8+ T cells from CD122−/− hosts. For experiments involving whole T cells, pooled LN cells from CD122$^{-/-}$ mice were subjected to complement-mediated killing by treating cell suspension with anti–heat-stable antigen mAb (J11d) and anti–MHC-II mAb (28-16-8s) plus complement (40). Purity was routinely >95%. Cells were then labeled

with CFSE (see above) and injected i.v. at $2–3 \times 10^6$ T cells per recipient. Recipients were irradiated with 750 cGy 6–8 h before adoptive transfer. For CD122$^{-/-}$ $CD8^+$ T cell subsets, LN cells from CD122$^{-/-}$ mice were prepared as described above and subsequently sorted by FACS. The purity of FACS-sorted $CD8^+ CD44^{hi}$ cells was ∼99%. Alternatively, CD122$^{-/-}$ $CD8^+$ cells were enriched for $CD44^{hi}$ cells by negative depletion of LN cells using MACS $CD8^+$ T cell isolation kit (Miltenyi Biotec) in combination with biotinylated anti-CD62L mAb (MEL-14). In brief, pooled LN cells from CD122$^{-/-}$ mice were incubated with biotinylated mAbs against CD4 (L3T4), CD45R (B220), CD49b (DX5), CD11b (Mac-1), Ter-119, and CD62L, followed by incubation with anti-biotin MicroBeads and negative depletion of labeled cells. Typical purities of sorted cells were ∼90%. CD122$^{-/-}$ $CD44^{hi}$ $CD8^+$ cells were then CFSE labeled and adoptively transferred i.v. at $2–3 \times 10^6$ cells per host. Recipient mice underwent split-dose irradiation of 600 cGy 2 wk before plus 600 cGy 6–8 h before adoptive transfer.

Mixed BM radiation chimeras. BM cells were obtained from Thy1.1-marked WT or MHC-I$^{-/-}$ mice, and mature B, T, and MHC-II–expressing cells were depleted using mAbs against heat-stable antigen (J11d), Thy1.1 (T24), CD4 (RL172), CD8 (3.168), and MHC-II (28-16-8s) plus complement. Contamination of purified BM cells with mature B, T, or MHC-II–expressing cells was <2%. Recipient Thy1.2-marked WT or MHC-I$^{-/-}$ mice were irradiated at 1,300 cGy before i.v. injection of $5–10 \times 10^6$ purified BM cells. Recipients were given antibiotics in their drinking water for the first 3–4 wk and left for 3–4 mo to allow for de novo T cell generation. Donor BM–derived T cells were then identified by Thy1.1 and purified using mAbs against heat-stable antigen (J11d), Thy1.2 (J1j.10), and MHC-II (28-16-8s) plus complement as described above. $2–3 \times 10^6$ Thy1.1 T cells were injected i.v. into Thy1.2 WT or MHC-I$^{-/-}$ mice, which had been depleted of NK cells using anti-NK1.1 ascites fluid (PK136) on days −3 and −1 before adoptive transfer and every other day thereafter.

Online supplemental material. Fig. S1 shows expression of CD25, CD122, γ_c, CD43, CD44, CD62L, CD69, and CD127 on antigen-specific naive, effector, and memory $CD8^+$ T cells during a response to lymphocytic choriomeningitis virus. Fig. S2 shows that, in vitro, IL-15 leads to down-regulation of CD122 on MP $CD8^+$ cells without affecting their CD62L levels. Fig. S3 shows that $CD8^+$ MP cells from CD122$^{-/-}$ mice are comparable to the $CD122^{lo}$ subset of MP $CD8^+$ cells from WT mice. Fig. S4 shows Vβ TCR usage within $CD8^+$ T cell subsets and within $CD8^+$ T cells undergoing homeostatic expansion. Figs. S1–S4 are available at http://www.jem.org/cgi/content/full/jem.20052495/DC1.

REFERENCES

1. Sprent, J., and C.D. Surh. 2002. T cell memory. *Annu. Rev. Immunol.* 20:551–579.

2. Bradley, L.M., L. Haynes, and S.L. Swain. 2005. IL-7: maintaining T-cell memory and achieving homeostasis. *Trends Immunol.* 26:172–176.

3. Seder, R.A., and R. Ahmed. 2003. Similarities and differences in CD4+ and CD8+ effector and memory T cell generation. *Nat. Immunol.* 4:835–842.

4. Sallusto, F., J. Geginat, and A. Lanzavecchia. 2004. Central memory and effector memory T cell subsets: function, generation, and maintenance. *Annu. Rev. Immunol.* 22:745–763.

5. Tan, J.T., E. Dudl, E. LeRoy, R. Murray, J. Sprent, K.I. Weinberg, and C.D. Surh. 2001. IL-7 is critical for homeostatic proliferation and survival of naive T cells. *Proc. Natl. Acad. Sci. USA.* 98:8732–8737.

6. Swain, S.L., H. Hu, and G. Huston. 1999. Class II–independent generation of CD4 memory T cells from effectors. *Science*. 286:1381–1383.

7. Grandjean, I., L. Duban, E.A. Bonney, E. Corcuff, J.P. Di Santo, P. Matzinger, and O. Lantz. 2003. Are major histocompatibility complex molecules involved in the survival of naive CD4$^+$ T cells? *J. Exp. Med*. 198:1089–1102.

8. Seddon, B., P. Tomlinson, and R. Zamoyska. 2003. Interleukin 7 and T cell receptor signals regulate homeostasis of CD4 memory cells. *Nat. Immunol*. 4:680–686.

9. Kondrack, R.M., J. Harbertson, J.T. Tan, M.E. McBreen, C.D. Surh, and L.M. Bradley. 2003. Interleukin 7 regulates the survival and generation of memory CD4 cells. *J. Exp. Med*. 198:1797–1806.

10. Lenz, D.C., S.K. Kurz, E. Lemmens, S.P. Schoenberger, J. Sprent, M.B. Oldstone, and D. Homann. 2004. IL-7 regulates basal homeostatic proliferation of antiviral CD4+ T cell memory. *Proc. Natl. Acad. Sci. USA*. 101:9357–9362.

11. Schluns, K.S., W.C. Kieper, S.C. Jameson, and L. Lefrancois. 2000. Interleukin-7 mediates the homeostasis of naive and memory CD8 T cells in vivo. *Nat. Immunol*. 1:426–432.

12. Tanchot, C., F.A. Lemonnier, B. Perarnau, A.A. Freitas, and B. Rocha. 1997. Differential requirements for survival and proliferation of CD8 naive or memory T cells. *Science*. 276:2057–2062.

13. Judge, A.D., X. Zhang, H. Fujii, C.D. Surh, and J. Sprent. 2002. Interleukin 15 controls both proliferation and survival of a subset of memory-phenotype CD8$^+$ T cells. *J. Exp. Med*. 196:935–946.

14. Kieper, W.C., J.T. Tan, B. Bondi-Boyd, L. Gapin, J. Sprent, R. Ceredig, and C.D. Surh. 2002. Overexpression of interleukin (IL)-7 leads to IL-15–independent generation of memory phenotype CD8$^+$ T cells. *J. Exp. Med*. 195:1533–1539.

15. Becker, T.C., E.J. Wherry, D. Boone, K. Murali-Krishna, R. Antia, A. Ma, and R. Ahmed. 2002. Interleukin 15 is required for proliferative renewal of virus-specific memory CD8 T cells. *J. Exp. Med*. 195:1541–1548.

16. Murali-Krishna, K., L.L. Lau, S. Sambhara, F. Lemonnier, J. Altman, and R. Ahmed. 1999. Persistence of memory CD8 T cells in MHC class I-deficient mice. *Science*. 286:1377–1381.

17. Zhang, X., S. Sun, I. Hwang, D.F. Tough, and J. Sprent. 1998. Potent and selective stimulation of memory-phenotype CD8+ T cells in vivo by IL-15. *Immunity*. 8:591–599.

18. Marks-Konczalik, J., S. Dubois, J.M. Losi, H. Sabzevari, N. Yamada, L. Feigenbaum, T.A. Waldmann, and Y. Tagaya. 2000. IL-2-induced activation-induced cell death is inhibited in IL-15 transgenic mice. *Proc. Natl. Acad. Sci. USA*. 97:11445–11450.

19. Fehniger, T.A., K. Suzuki, A. Ponnappan, J.B. VanDeusen, M.A. Cooper, S.M. Florea, A.G. Freud, M.L. Robinson, J. Durbin, and M.A. Caligiuri. 2001. Fatal leukemia in interleukin 15 transgenic mice follows early expansions in natural killer and memory phenotype CD8$^+$ T cells. *J. Exp. Med*. 193:219–231.

20. Kennedy, M.K., M. Glaccum, S.N. Brown, E.A. Butz, J.L. Viney, M. Embers, N. Matsuki, K. Charrier, L. Sedger, C.R. Willis, et al. 2000. Reversible defects in natural killer and memory CD8 T cell lineages in interleukin 15–deficient mice. *J. Exp. Med*. 191:771–780.

21. Lodolce, J.P., D.L. Boone, S. Chai, R.E. Swain, T. Dassopoulos, S. Trettin, and A. Ma. 1998. IL-15 receptor maintains lymphoid homeostasis by supporting lymphocyte homing and proliferation. *Immunity*. 9:669–676.

22. Tough, D.F., and J. Sprent. 1994. Turnover of naive- and memory-phenotype T cells. *J. Exp. Med*. 179:1127–1135.

23. Seaman, M.S., B. Perarnau, K.F. Lindahl, F.A. Lemonnier, and J. Forman. 1999. Response to Listeria monocytogenes in mice lacking MHC class Ia molecules. *J. Immunol*. 162:5429–5436.

24. Tan, J.T., B. Ernst, W.C. Kieper, E. LeRoy, J. Sprent, and C.D. Surh. 2002. Interleukin (IL)-15 and IL-7 jointly regulate homeostatic proliferation of memory phenotype CD8$^+$ cells but are not required for memory phenotype CD4$^+$ cells. *J. Exp. Med*. 195:1523–1532.

25. Tough, D.F., P. Borrow, and J. Sprent. 1996. Induction of bystander T cell proliferation by viruses and type I interferon in vivo. *Science*. 272:1947–1950.

26. Min, B., R. McHugh, G.D. Sempowski, C. Mackall, G. Foucras, and W.E. Paul. 2003. Neonates support lymphopenia-induced proliferation. *Immunity*. 18:131–140.

27. Ernst, B., D.S. Lee, J.M. Chang, J. Sprent, and C.D. Surh. 1999. The peptide ligands mediating positive selection in the thymus control T cell survival and homeostatic proliferation in the periphery. *Immunity*. 11:173–181.

28. Goldrath, A.W., and M.J. Bevan. 1999. Low-affinity ligands for the TCR drive proliferation of mature CD8+ T cells in lymphopenic hosts. *Immunity*. 11:183–190.

29. Pereira, P., L. Forni, E.L. Larsson, M. Cooper, C. Heusser, and A. Coutinho. 1986. Autonomous activation of B and T cells in antigen-free mice. *Eur. J. Immunol*. 16:685–688.

30. Min, B., H. Yamane, J. Hu-Li, and W.E. Paul. 2005. Spontaneous and homeostatic proliferation of CD4 T cells are regulated by different mechanisms. *J. Immunol*. 174:6039–6044.

31. Kieper, W.C., A. Troy, J.T. Burghardt, C. Ramsey, J.Y. Lee, H.Q. Jiang, W. Dummer, H. Shen, J.J. Cebra, and C.D. Surh. 2005. Recent immune status determines the source of antigens that drive homeostatic T cell expansion. *J. Immunol*. 174:3158–3163.

32. Wherry, E.J., V. Teichgraber, T.C. Becker, D. Masopust, S.M. Kaech, R. Antia, U.H. von Andrian, and R. Ahmed. 2003. Lineage relationship and protective immunity of memory CD8 T cell subsets. *Nat. Immunol*. 4:225–234.

33. Marzo, A.L., K.D. Klonowski, A. Le Bon, P. Borrow, D.F. Tough, and L. Lefrancois. 2005. Initial T cell frequency dictates memory CD8+ T cell lineage commitment. *Nat. Immunol*. 6:793–799.

34. Masopust, D., V. Vezys, A.L. Marzo, and L. Lefrancois. 2001. Preferential localization of effector memory cells in nonlymphoid tissue. *Science*. 291:2413–2417.

35. Wherry, E.J., D.L. Barber, S.M. Kaech, J.N. Blattman, and R. Ahmed. 2004. Antigen-independent memory CD8 T cells do not develop during chronic viral infection. *Proc. Natl. Acad. Sci. USA*. 101:16004–16009.

36. Klenerman, P., and A. Hill. 2005. T cells and viral persistence: lessons from diverse infections. *Nat. Immunol*. 6:873–879.

37. Zhou, S., R. Ou, L. Huang, G.E. Price, and D. Moskophidis. 2004. Differential tissue-specific regulation of antiviral CD8+ T-cell immune responses during chronic viral infection. *J. Virol*. 78:3578–3600.

38. Paiardini, M., B. Cervasi, H. Albrecht, A. Muthukumar, R. Dunham, S. Gordon, H. Radziewicz, G. Piedimonte, M. Magnani, M. Montroni, et al. 2005. Loss of CD127 expression defines an expansion of effector CD8+ T cells in HIV-infected individuals. *J. Immunol*. 174:2900–2909.

39. Boyman, O., M. Kovar, M.P. Rubinstein, C.D. Surh, and J. Sprent. 2006. Selective stimulation of T cell subsets with antibody–cytokine immune complexes. *Science*. 311:1924–1927.

40. Kosaka, H., C.D. Surh, and J. Sprent. 1992. Stimulation of mature unprimed CD8$^+$ T cells by semiprofessional antigen-presenting cells in vivo. *J. Exp. Med*. 176:1291–1302.